

Figure 28: Leg I basitarsus (150x), ventral view, showing characteristic spinule clusters. *Iurus asiaticus*, male, Kaşlıca, Adıyaman, Turkey.

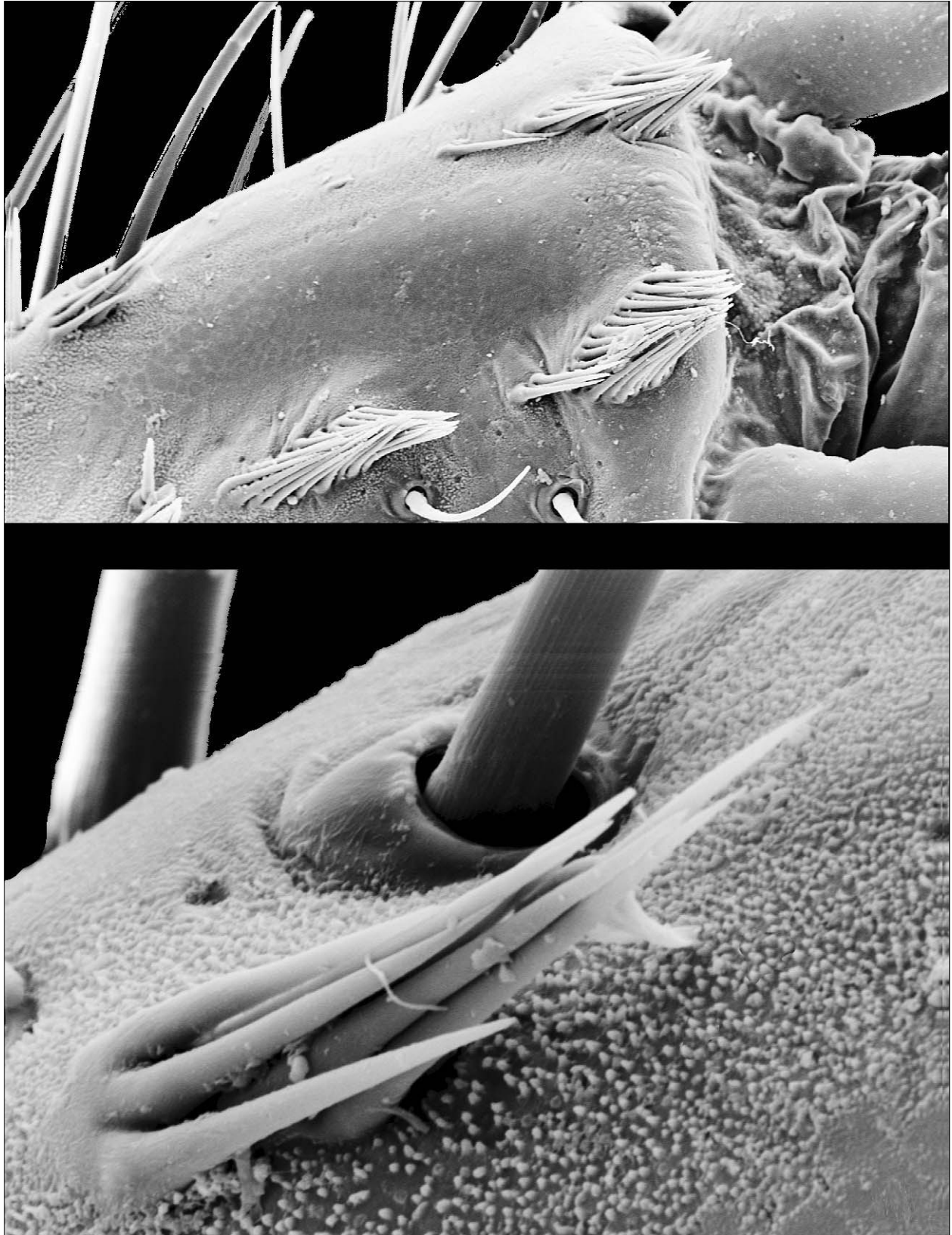


Figure 29: Leg I basitarsus, *Iurus kraepelini*, juvenile male, Akseki, Antalya, Turkey. **Top.** Distal aspect showing small spinule clusters (150x). **Bottom.** Close-up of spinule cluster (750x).

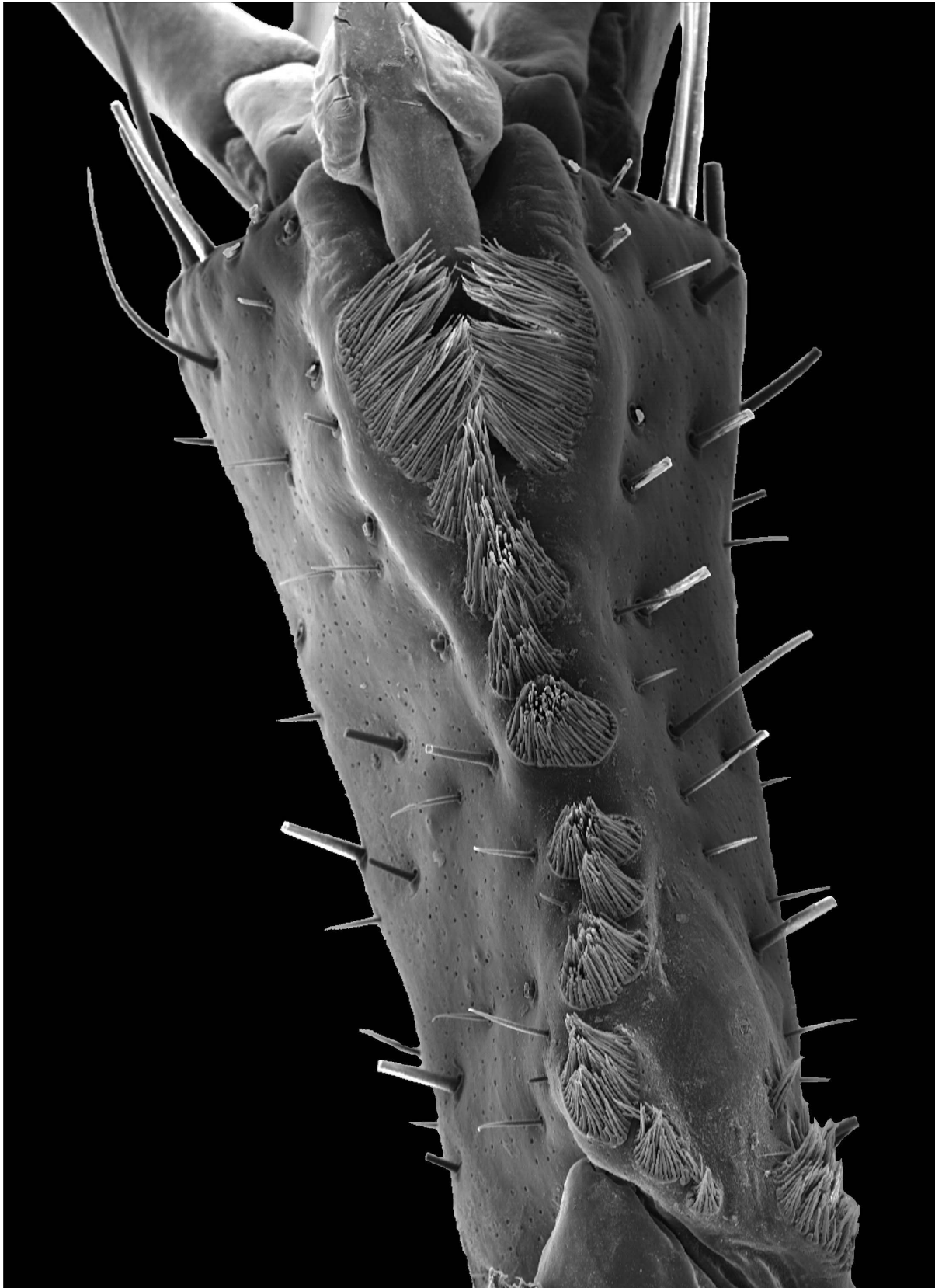


Figure 30: Leg I tarsus, adult *Iurus kraepelini*, Turkey, showing the well developed spinule clusters (50x) (after Fet et al., 2004: fig. 5, in part).

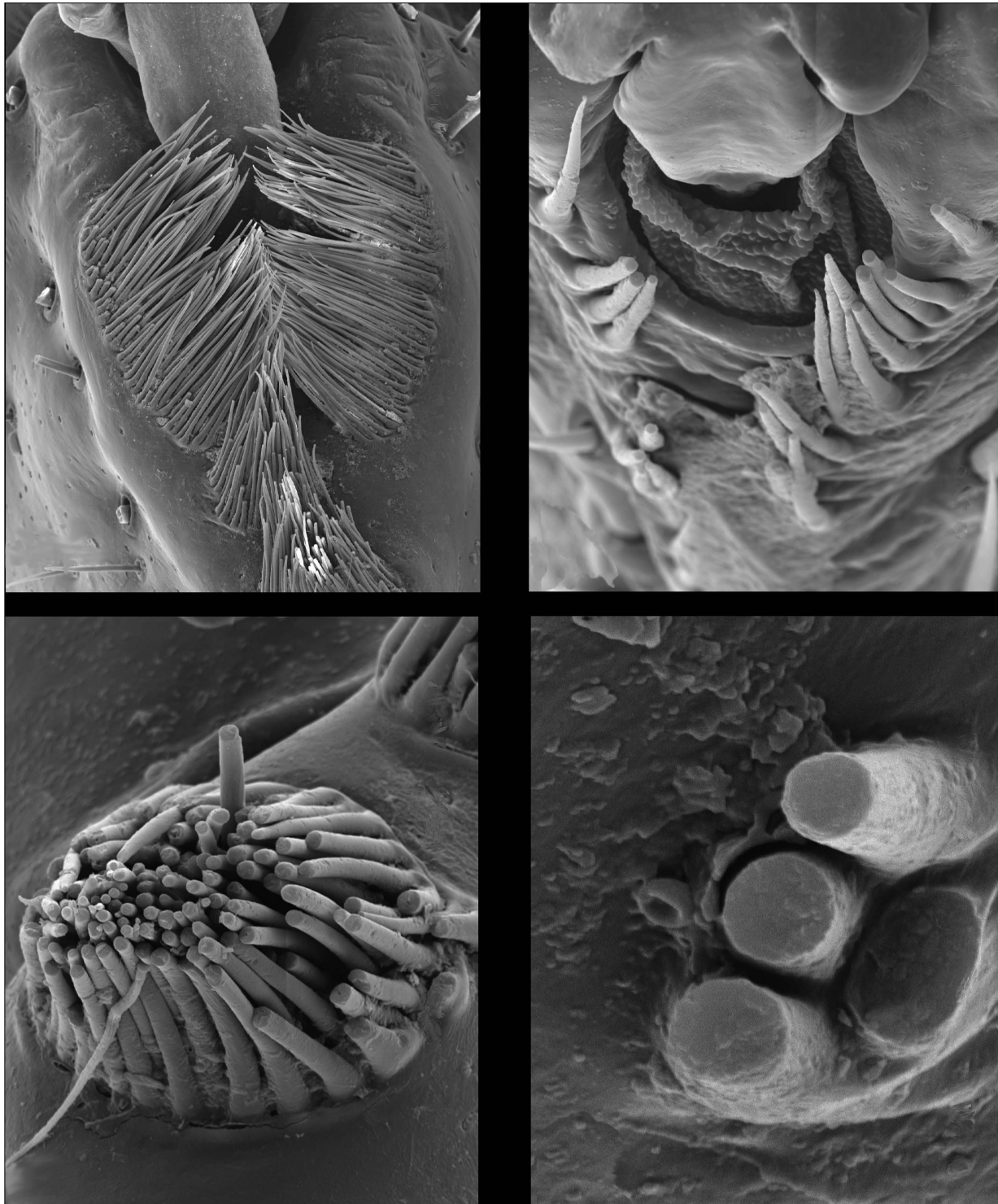


Figure 31: Closeup of leg tarsus showing significant differences in the development of the ventral spinule clusters between adult and juvenile *Iurus*. **Top.** Distal aspect of spinule clusters, adult male *I. kraepelini* (150x) (left), Turkey, compared to juvenile *I. dufourei* (750x) (right), Crete, Greece. **Bottom.** Individual spinule cluster of *I. dufourei*, adult female (750x) (left), Crete, Greece, compared to juvenile (3500x) (right), Crete, Greece. Note the distinctive blunted terminus of individual spinules, characteristic of *Iurus* (after Fet et al., 2004: figs. 6, 8, 38, 40).

vesicle, an extension of this sac, is found on the ventromedial section of the hemispermaphore with the vas deferens extending from its distal aspect (i.e., lamina

end). A hemispermaphore, when removed from its membranous sac, is yellowish in color with sclerotized substructures of a contrasting mahogany color. These

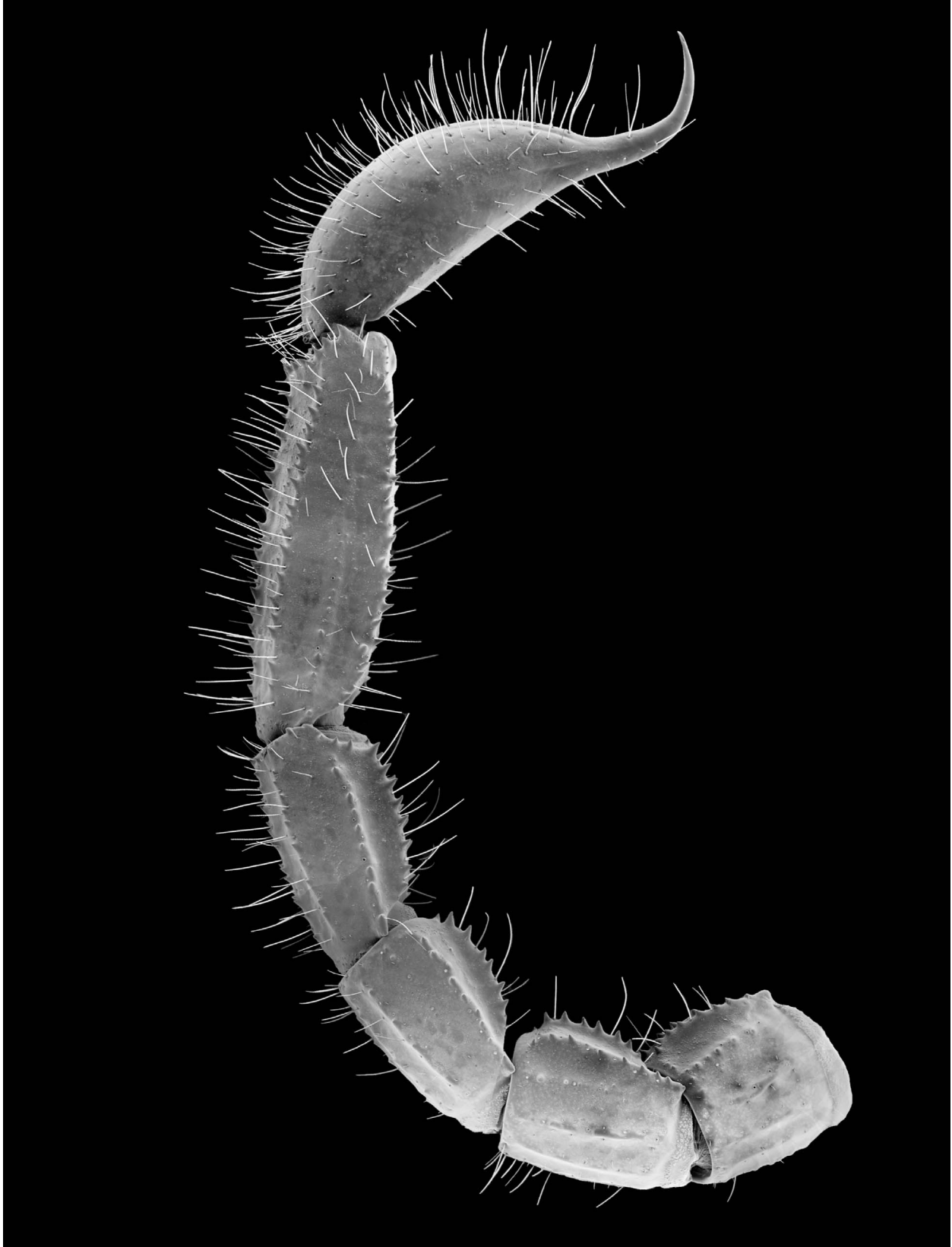


Figure 32: Metasoma and telson, lateral view (15x), *Iurus kraepelini*, juvenile male, Akseki, Antalya, Turkey.

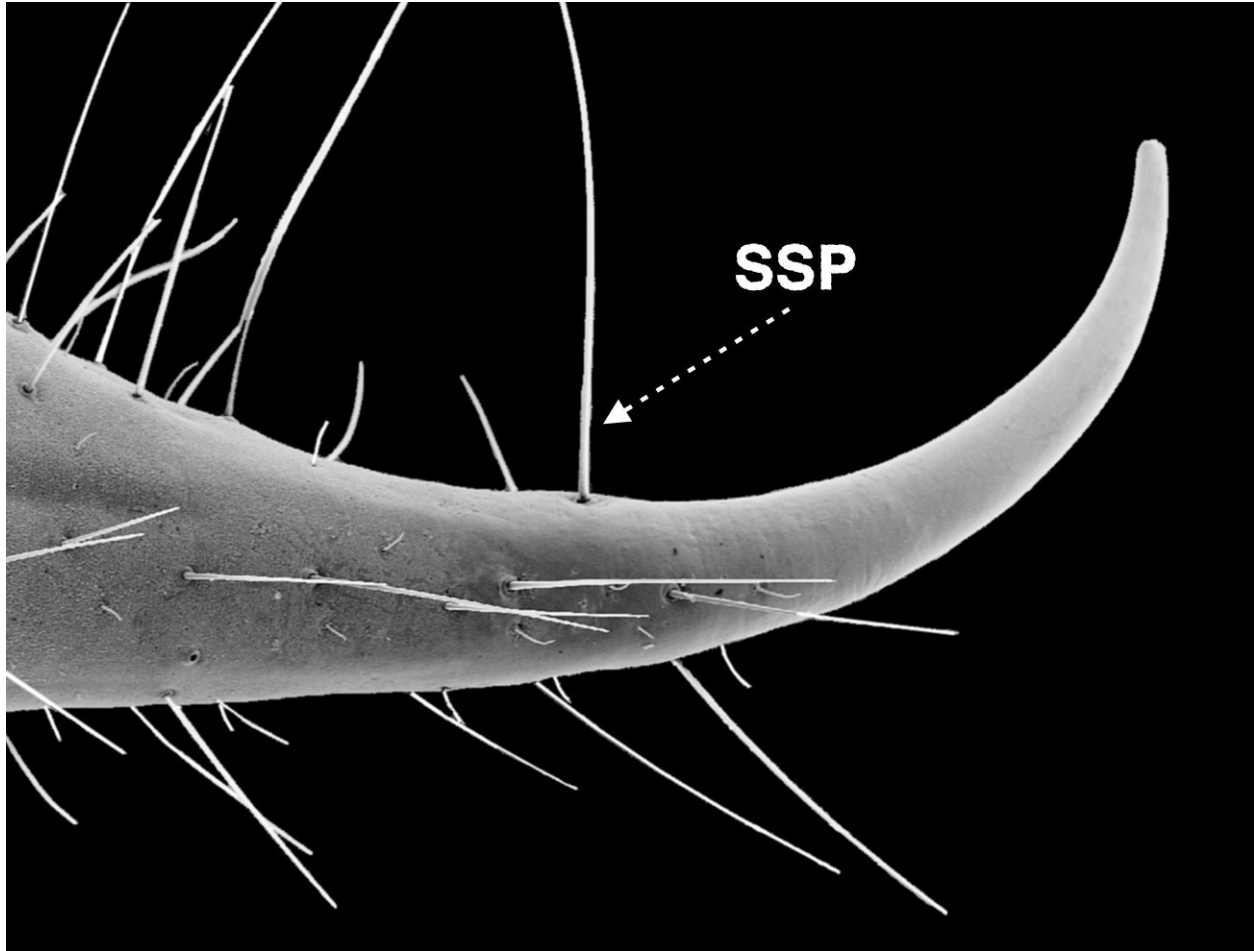


Figure 33: Aculeus, *Iurus dufourei*, subadult female, Krini, Gythio, Laconia, Greece, showing enlarged Subaculear Setal Pair (SSP) on aculeus midpoint (35x).

structures are 10–13 mm long. The hemispermatophore of *Iurus* is composed of three sections (Fig. 42): the *trunk*, the *median area*, and the *lamina*.

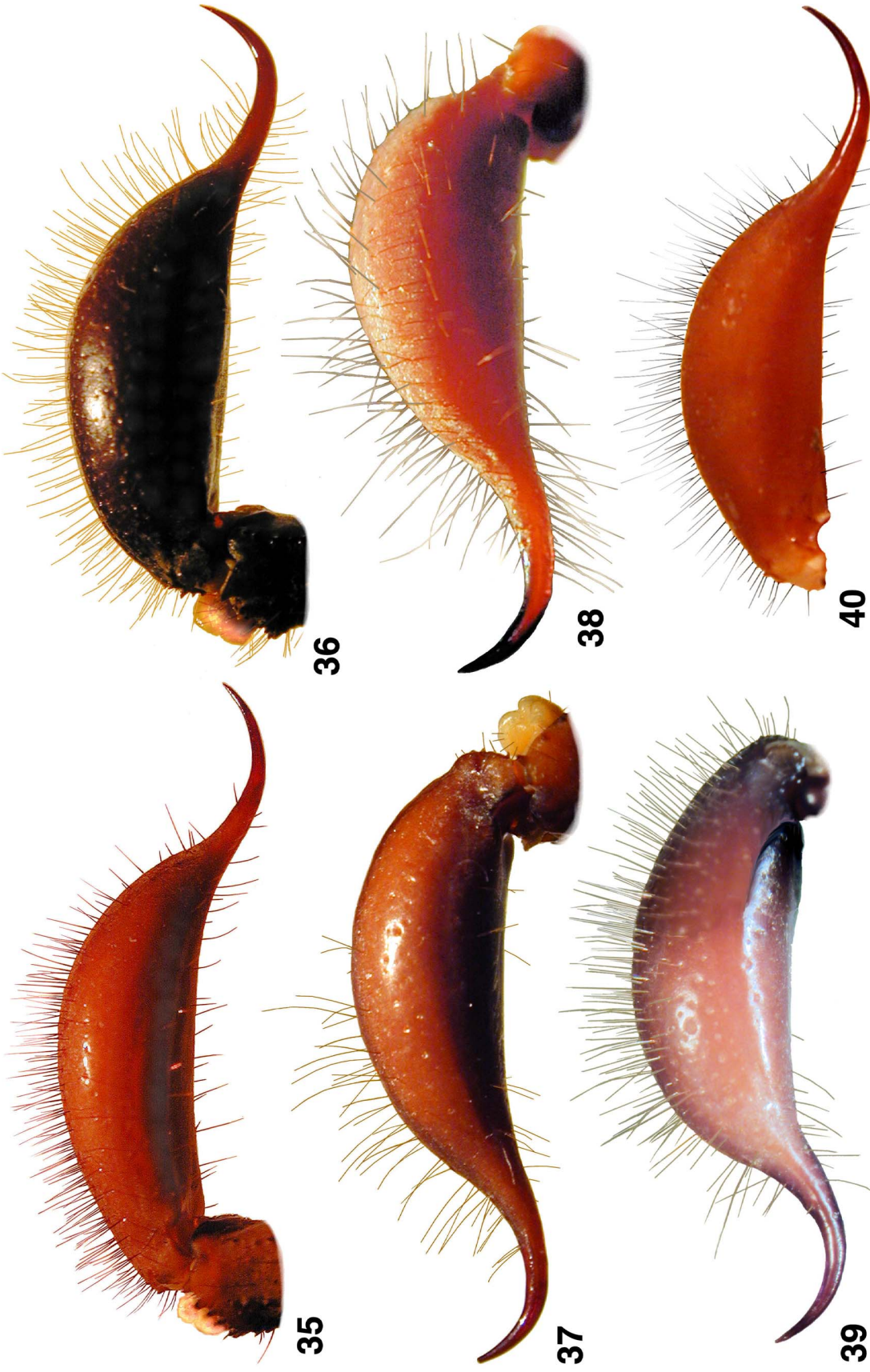
The **trunk** is a somewhat complex structure, wide and bulbous at the median area and tapering considering into a somewhat pointed “foot”. The bulbous section is highly convex on the dorsal side and equally concave ventrally. The actual walls of the trunk are thin slightly sclerotized cuticle supported by thickened bolsters (termed “ribs” by Lamoral, 1979). These bolsters are highly sclerotized, mahogany in color, thus contrasting with the lighter yellowish trunk walls. All hemispermatophores examined in this study exhibited at least two bolsters, a *primary bolster*, which traverses vertically from the base of the bulbous section to the foot’s external edge, and a *secondary bolster*, which extends down the internal edge from the base of the bulbous section to the trunk’s midpoint. In some *Iurus* species, *transverse bolsters* are also present. These bolsters extend horizontally from the medial area of the primary

bolster towards the internal edge. Two to four transverse bolsters have been observed in this study.

The **median area** is where the lamina connects to the trunk, formed by the *dorsal* and *ventral troughs*. The *acuminate process* and *seminal receptacle* are also located in the median area. On the external edge of the median area is a conspicuously developed *truncal flexure*. The **acuminate process** is a conspicuous mahogany colored highly sclerotized hook-like structure that originates from the internal edge of the median area, just above the dorsal/ventral troughs, curving in an upward/dorsal direction. The acuminate process tapers from its base to a somewhat pointed terminus, which is usually truncated, though a blunted terminus is found in one species. On the ventral side of the median area is the **seminal receptacle**, a sclerotized, mahogany-colored semicircular process found just above the ventral trough edge. Since most of the hemispermatophore is yellowish in color and translucent, highly sclerotized substructures such as the seminal receptacle or bolsters show through on the opposite surface. Therefore, this receptacle is



Figure 34: Telson, lateral view, showing subaculear setal pair (SSP) on *Jurus dufourei*, juvenile female, Mystras, Laconia, Greece. Note location of SSP on midpoint of the aculeus.



Figures 35–40: Telson of *Iurus*, lateral view. **35.** *I. kadleci*, sp. nov., adult male, Akseki, Antalya, Turkey. **36.** *I. kraepelini*, adult male, Akseki, Antalya, Turkey. **37.** *I. kinzelbachii*, sp. nov., adult male, Naldöken ("Narli Kioi"), Izmir, Turkey. **38.** *I. dufourei*, adult male, Selimitsa, Greece. **39.** *I. asiaticus*, adult male, Çamlıyayla, Mersin, Turkey. **40.** *I. kadleci*, subadult female, Dim Cave, Antalya, Turkey.

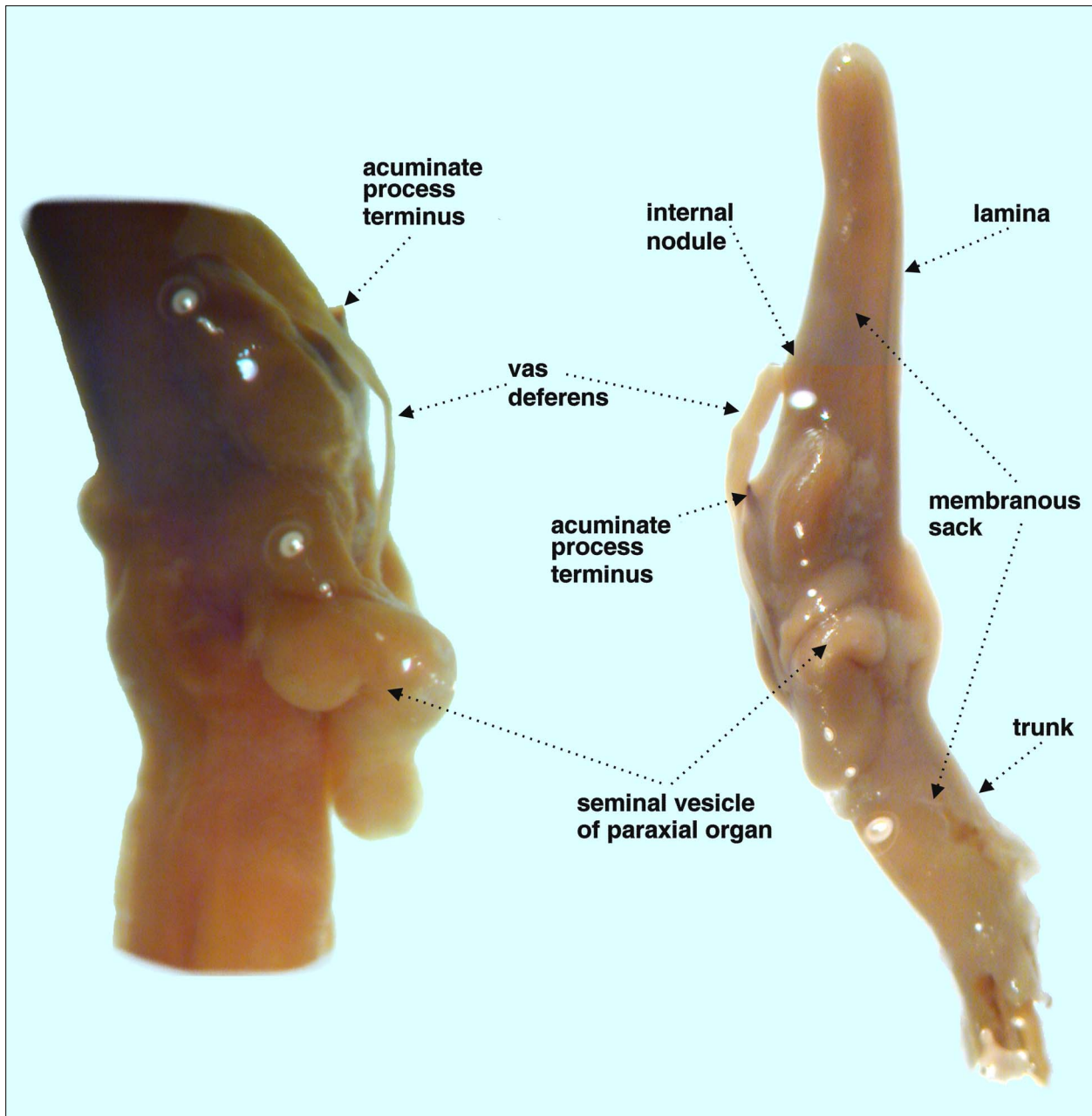


Figure 41: Right hemispermatochore of *Jurus asiaticus*, ventrointernal view, showing membranous sack, and the attachment of the paraxial organ and severed vas deferens. **Right.** Yaylaüstü Village, Central District, Kahramanmaraş, Turkey, showing entire hemispermatochore with major components identified. **Left.** Kaşlıca, Adıyaman, Turkey, showing a close-up of the paraxial organ seminal vesicle and vas deferens (this partial image is reversed for comparison). Note that the entire hemispermatochore is enclosed in a sarcophagus-like membranous sack. The highly sclerotized terminus of the acuminate process is partially visible through the membrane in both photographs.

quite visible from the dorsal surface. This semi-circular receptacle ridge creates a hollow with the ventral trough edge (discussed further below). In many hemispermatochores examined, a somewhat fragile transparent structure was found attached to the internal edge of the seminal receptacle, termed here the **paraxial organ**

sleeve. We hypothesize that this sleeve forms a conduit between the paraxial organ seminal vesicle and the seminal receptacle.

The **lamina** originates from the median area, its base formed by the dorsal and ventral troughs. With little sclerotization, the lamina is somewhat translucent.

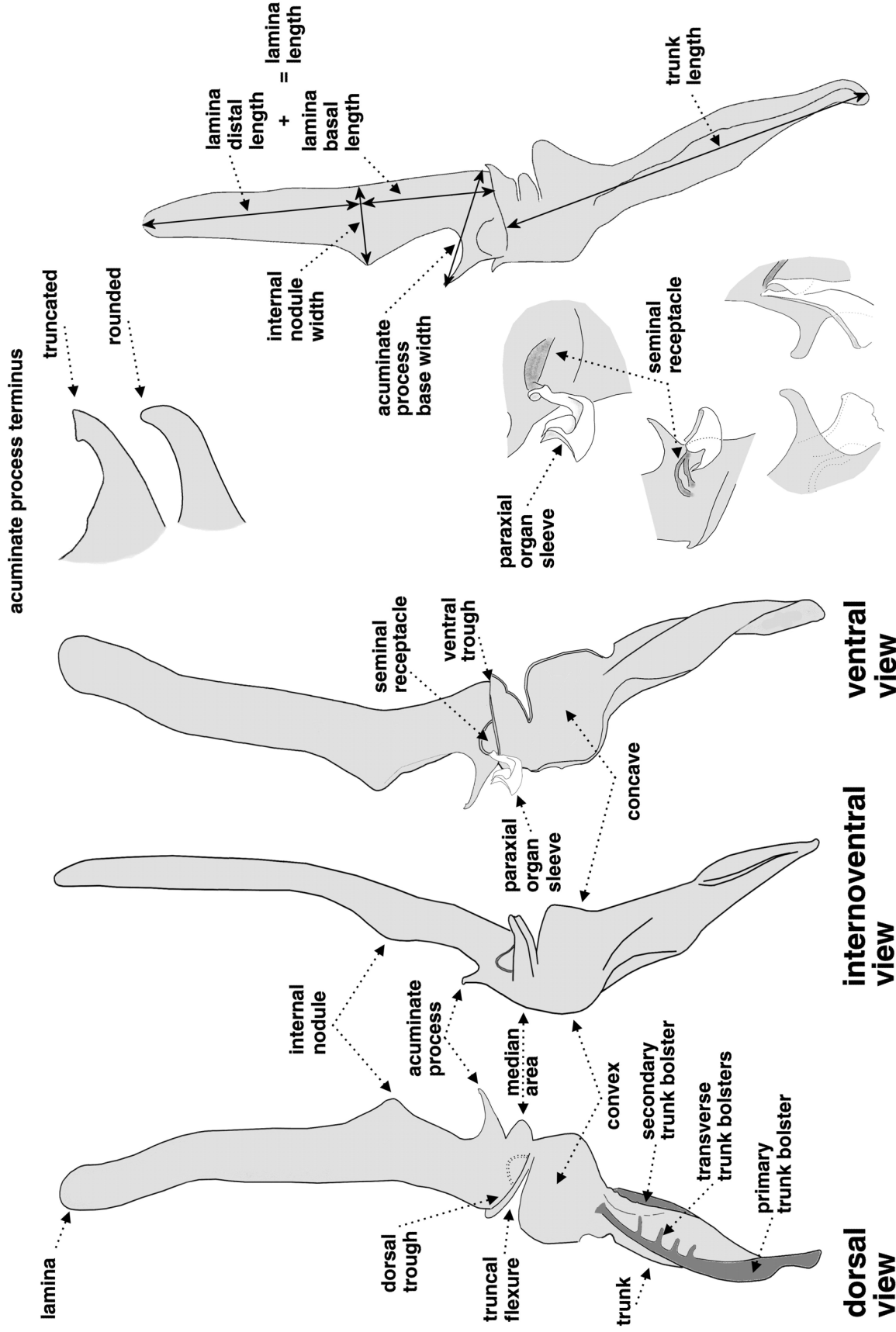


Figure 42: *Iurus* hemispermatophore. Terminology and method of measurement (from a right hemispermatophore perspective).

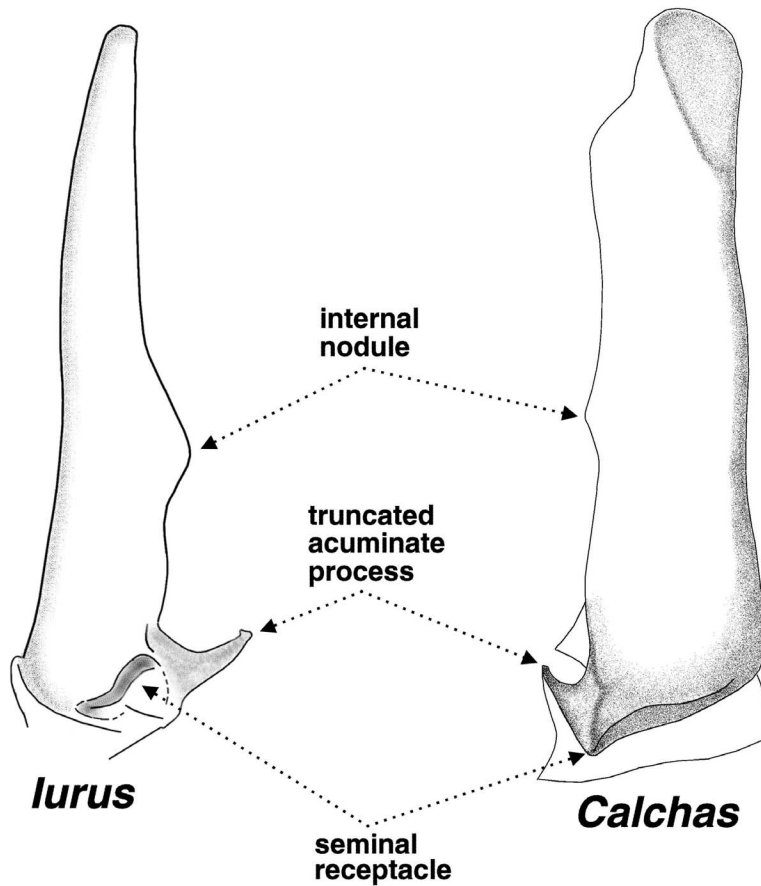


Figure 43: Hypothesized homologies for hemispermatophore morphology in genera *Iurus* and *Calchas*. Only lamina and median areas shown.

Though depending on the species, the lamina typically tapers distally, its terminus usually being narrower than the other areas. Present in all species examined is an **internal nodule** located on the internal edge, positioned on the proximal half of the lamina. The exact shape of this nodule and its relative position on the lamina is species-specific. The internal nodule extends the furthest on the internal edge, the lamina base and terminus subtly angling externally, the nodule forming the apex.

When viewing the hemispermatophore from either the internal or external edges, the median area angles outward in a dorsal direction, the lamina terminus and trunk foot pointing in a ventral direction, thus forming an obtuse angle roughly 135° (i.e., the median area as the apex).

Sperm transfer. From the above description of the *Iurus* hemispermatophore, it is clear that this is a somewhat simplistic and primitive form of the lamelliform type. There is no complex capsule as found in many lamelliform type scorpions, no mating plug as found in the vaejovids, or a multitude of complex lobe structures as identified in many scorpionoids, etc. The actual sequence of sperm transfer in this type of

hemispermatophore is not known. However, it appears that the sperm from the testes is transferred directly to the paraxial organ seminal vesicle via the vas deferens and then deposited into the seminal receptacle. There are two components of this receptacle, the outer sclerotized semi-circular ridge, and the hollow formed by this ridge and the ventral trough edge. As of now, we do not know where the sperm is actually deposited, but we can hypothesize two scenarios: 1) the semi-circular ridge is hollow and the sperm is injected into this sclerotized ridge (i.e., the ridge orifice would be the “sperm duct”); 2) the sperm is deposited into the hollow formed by the ridge and ventral trough. The latter scenario would only make sense if the two hemispermatophores (left and right) are “glued” together before the injection of sperm, thus forming an enclosed compartment to hold the sperm. The attachment of the paraxial organ sleeve can support either scenario of sperm transfer.

Comparison to *Calchas*. The hemispermatophore trunk is quite different between *Iurus* and *Calchas*. In the former, we have a sclerotized contorted structure exhibiting convoluted convex and concave contours whereas in the latter, the trunk is an evenly rounded membraneous non-sclerotized component that tapers to a

point at its foot. A truncal flexure is found in both genera, moderately developed in *Calchas* and conspicuous in *Iurus*. The lamina in *Iurus* generally tapers from its base to a narrower distal tip, whereas in *Calchas* the lamina is spatulate in form, the lateral edges subparallel, the terminus abruptly truncated (Fig. 43). Both genera exhibit an **acuminate process** with a truncated terminus, unprecedented in Recent scorpions. In *Iurus*, this process is longer, protruding further from the median area. On the internal edge of the proximal half of the lamina is an **internal nodule** found in both genera. In *Iurus*, this nodule is variable in its relative location on the lamina, its width, size, and overall shape, species dependent. In *Calchas* (based on two species), the internal nodule is a subtle small pointed projection located just proximally of lamina midpoint. Both genera have a simplistic **seminal receptacle** located on the ventral surface just above the ventral trough. In *Iurus*, the receptacle is highly sclerotized, and therefore pigmented, forming a conspicuous semi-circle above the ventral trough. The receptacle in *Calchas* is not overly sclerotized or conspicuous; its upper edge forms a small slit-like hollow with the ventral trough edge. Unique to *Calchas* is a curious non-sclerotized triangular **internal protuberance** located on the internal edge of the lamina base. This protuberance is situated closer to the dorsal surface, thus not directly on the internal edge.

We consider the acuminate process (with truncated terminus), internal nodule, and the seminal receptacle to be *homologous structures* between these two genera and probable *synapomorphies* for family Iuridae (see Fig. 43). Of course, a detailed analysis of all iuroid hemispermatophore morphology and comparison to putative outgroup *Chaerilus* needs to be conducted in order to substantiate this hypothesis (Soleglad et al., in progress).

Species-Level Comparisons

In this section, major characters used to separate *Iurus* species are discussed in detail including an illustrated key. The major structures separating the five species currently recognized in *Iurus* include the morphology of the pedipalp chela and hemispermatophore, and several morphometrics. Other characters such as number of chelal finger inner denticles (*ID*), neobothriotaxy, and pectinal tooth counts are also discussed.

Illustrated key to species of *Iurus*

1 - Lobe position of chelal movable finger in adults basal of midfinger, lobe ratio 0.38–0.47 (Fig. 56); inner denticles (*ID*) of chelal movable finger number 14–16 (14.42) (Tab. 1); hemispermatophore transverse trunk bolsters present (Figs. 98, 216), lamina terminus rounded (Figs. 61–63), and lamina distal length / basal

length = 3.4–4.7 (Tab. 2); pectinal tooth counts 10–11 (10.63) males, 9–11 (9.58) females (Fig. 73) **2**

■ - Lobe position of chelal movable finger in adults midfinger or distal, lobe ratio 0.44–0.64 (Fig. 56); inner denticles (*ID*) of chelal movable finger number 11–13 (12.45) (Tab. 1); hemispermatophore transverse trunk bolsters absent (Figs. 132, 168), lamina terminus pointed (Figs. 64–72), and lamina distal length / basal length = 1.7–2.6 (Tab. 2); pectinal tooth counts 11–14 (12.49) males, 10–12 (11.38) females (Fig. 73) **3**

2 - Proximal gap lacking on chelal fixed finger in adult males (Fig. 59); hemispermatophore internal nodule conspicuous and knob-shaped, acuminate process terminus truncated (Fig. 61), and lamina length / internal nodule width = 6.8; chela fixed finger length / telson width = 2.62–2.73 males, 2.64–2.96 females, and movable finger length / telson width = 3.21–3.40 males, 3.31–3.68 females (Fig. C3) ***I. dufourei* (Brullé, 1832)**

■ - Proximal gap present on chelal fixed finger in adult males (Fig. 59); hemispermatophore internal nodule weak to obsolete, acuminate process terminus rounded (Fig. 62), lamina length / internal nodule width = 8.7; chela fixed finger length / telson width = 3.37–3.46 males, 3.41–3.65 females, and movable finger length / telson width = 4.14–4.34 males, 4.26–4.32 females (Fig. C3) ***I. kinzelbachi* sp. nov.**

3 - Proximal gap of chelal fixed finger vestigial to obsolete in adult females (Figs. 127, 163); metasomal segments stocky (Figs. C4–C5), segments I–III length / width = 0.81–0.92, 1.04–1.17, 1.24–1.37 males, 0.70–0.85, 0.97–1.11, 1.15–1.34 females; telson vesicle relatively wide (Fig. C3), telson length / vesicle width = 3.18–3.67 males, 3.27–3.49 females; dark grey to black in color (Figs. 110, 149) **4**

■ - Proximal gap of chelal fixed finger large and conspicuous in adult females (Fig. 194); metasomal segments slender, all longer than wide (Figs. C4–C5), segments I–III length / width = 1.10–1.28, 1.35–1.45, 1.64–1.69 males, 1.11–1.12, 1.36–1.55, 1.55–1.71 females; telson vesicle narrow (Fig. C3), telson length / vesicle width = 4.34 males, 3.98–4.34 females; light reddish in color with darker chelae (Fig. 182) ***I. kadleci* sp. nov.**

4 - In adult males proximal gap of chelal fixed finger exaggerated, movable finger highly curved, and chelal palm short, noticeably vaulted (Figs. 121–126); chela depth / chela length = 0.41–0.46 males, 0.37–0.38 females (Fig. C2); hemispermatophore internal nodule widely rounded, located basally on lamina, lamina distal length / basal length = 2.16–3.07 (Tab. 2)..... ***I. kraepelini* von Ubisch, 1922**

■ - In adult males, proximal gap of chelal fixed finger not exaggerated, movable finger essentially straight with

a subtle curve, chelal palm elongated, not vaulted (Figs. 159–162); chela depth / chela length = 0.32–0.35 males, 0.32–0.34 females (Fig. C2); hemispermatophore internal nodule pointed, located suprabasally on lamina, lamina distal length / basal length = 1.61–1.80 (Tab. 2) *I. asiaticus* Birula, 1903

(note that *standard error* ranges are stated in the above key)

Major morphological differences between *Iurus* species

The pedipalp chela and hemispermatophore provide major diagnostic characters for separating the five species we recognize in genus *Iurus*. However, it is important to note that the diagnostic characters derived from these two structures are based only on sexually mature males. Other important diagnostic characters, morphometrics in particular, also depend on mature specimens, but do include both genders. Fortunately, the morphometrics identified herein as diagnostic apply equally to both male and female. Lesser characters, such as the number of inner denticles (*ID*) of the movable finger, or number of pectinal teeth, are relevant for juvenile and subadult specimens as well as for adults.

Pedipalp chela morphology

Chelal finger lobe/socket and the proximal gap. Francke (1981), in a small but important paper on *Iurus*, was the first to observe the taxonomic value of the movable finger lobe in this genus. Although the material he studied was quite limited, Francke was able to identify some of the key issues concerning the lobe's structure, its bearing on sexual dimorphism, and allometric growth.

We examined the movable finger (MF) lobe of the chela from several perspectives: its relationship to the fixed finger socket and proximal gap if present; the relative position of the lobe on the movable finger; differences in form and location based on sexual dimorphism; development and relative finger lobe position with respect to allometric growth; and its overall importance to *Iurus* taxonomy. This examination of the MF lobe involved the study of over 200 specimens.

Lobe/socket relationships. Among Iuridae, a lobe on the denticle surface of the movable finger is present only in *Iurus* (this lobe is absent in its sister genus *Calchas*). This lobe increases in size and shape as the scorpion matures. Corresponding to this lobe is a socket (also called “notch” in literature) on the fixed finger which allows the denticle edges to meet when the fingers are closed. In Figures 44–55, we illustrate two basic configurations of chelal finger lobe/socket arrangement.

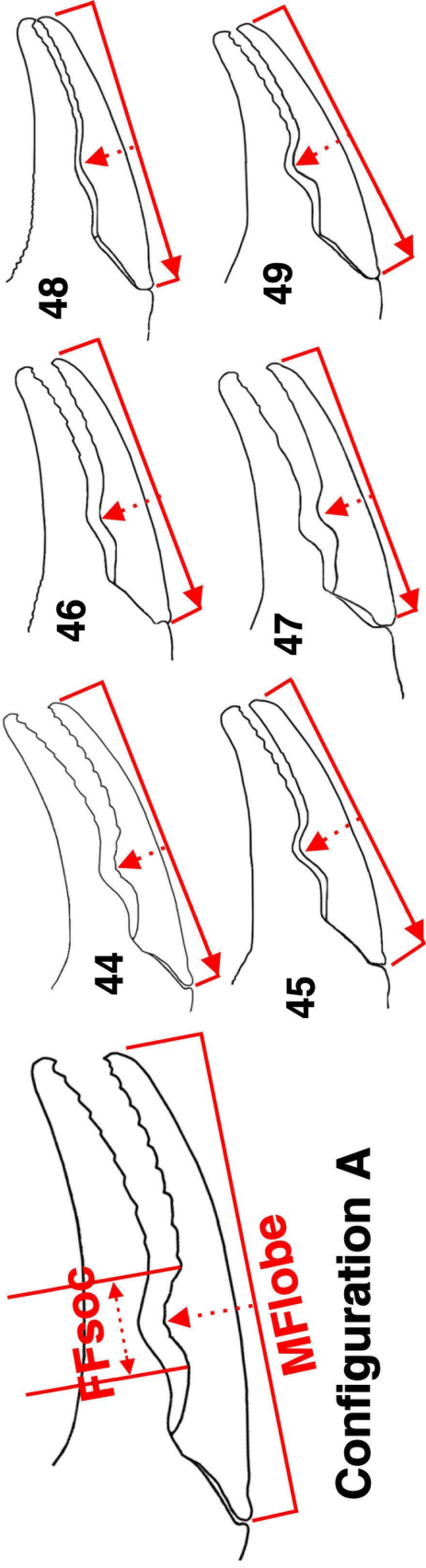
In configuration A, the socket and lobe have the same basal width, the lobe fitting exactly into the socket when the two fingers are closed. In configuration B, the socket base is wider than the lobe base, sometimes exceeding its width by a factor of two. The increase in socket width occurs proximally, the distal part of the socket matching up with the lobe when the fingers are closed. Therefore, when the fingers are closed there is a conspicuous gap between the fingers proximal of the MF lobe, termed in this paper a *proximal gap*. Figures 44–55 illustrates diagrammatically the lobe/socket relationship for both configurations, spanning all recognized *Iurus* species. In addition, a multitude of lateral views of chelae are presented under the individual species descriptions for all species examined in this study, for both males and females.

In general, configuration B is only detectable in large sexually mature males, and is not usually apparent in females. A notable exception is *I. kadleci*, **sp. nov.**, where the adult female exhibits a conspicuous proximal gap (this is discussed further below).

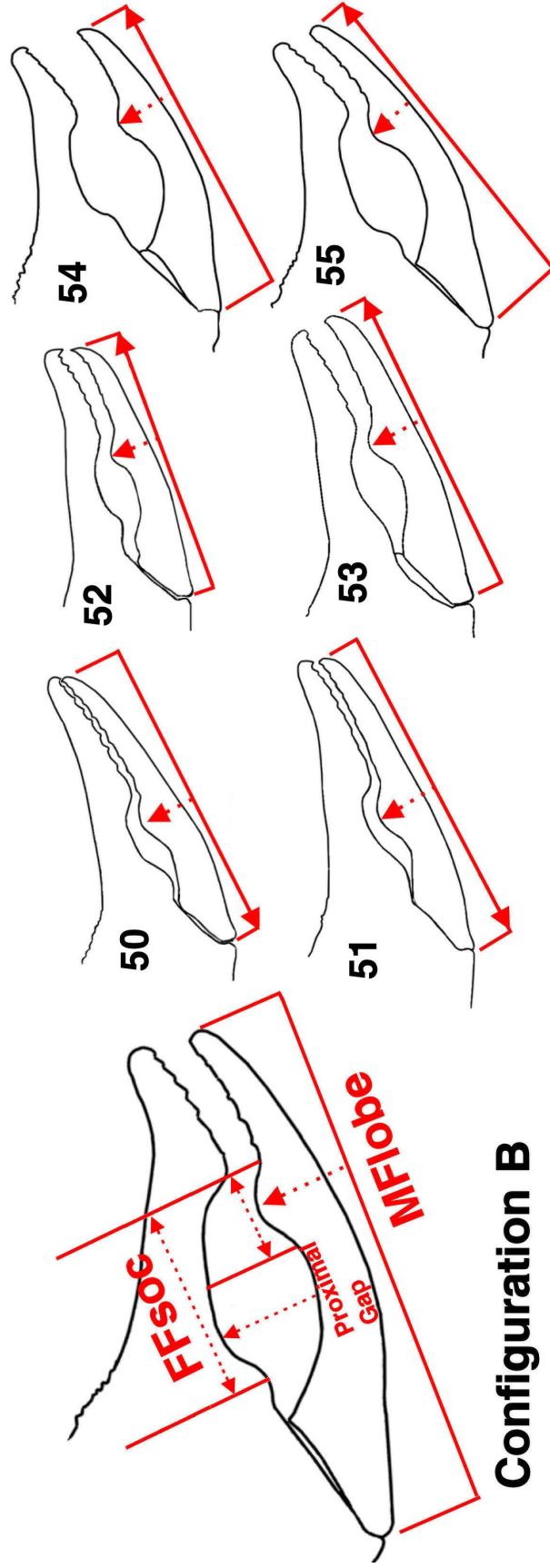
Lobe location on movable finger. Of particular interest for the MF lobe is its relative position on the finger. In the scatter chart shown in Fig. 56, the MF lobe ratio is analyzed with respect to the specimen's size, as represented by its carapace length. The ratio is the distance from the lobe to the external condyle divided by the movable finger length (see Fig. 57 for exact methods of measurement), thus representing its relative position on the finger; i.e., ratio < 0.5 = lobe proximal of midfinger, ratio > 0.5 = lobe distal of midfinger. Two attributes of this analysis are readily apparent directly from the scatter chart: 1) the lobe is found more distally on larger specimens within a species; 2) the species are partitioned into two groups, in part, by their lobe's relative position on the finger.

In Fig. 56 we see that the distribution of the various colored icons angles upwards as the MF lobe ratio increases (which means a lobe occurring further on the finger). This implies that the lobe does indeed occur further on the finger on larger specimens than it does on smaller specimens (as indicated by carapace length). For example, the smallest specimen of *I. dufoureyus* examined has a carapace of 6.9 mm and a lobe ratio of 0.317, also the smallest obtained in this species. In contrast, the largest specimen examined, with a carapace of 13 mm, exhibits the largest lobe ratio, 0.458. We see a similar condition in *I. kraepelini* (our largest dataset), where the smallest specimen has a carapace of 7.2 mm and a lobe ratio of 0.400, and nine specimens with the largest lobe ratios, 0.600 to 0.637, have carapaces ranging 11.85 to 14.65.

The separation of five species into two groups is clear in Fig. 56, as indicated by “red” + “blue”, and “green” + “black” + “white” icons, respectively. This can be verified by inspecting the histogram in Fig. 56



Configuration A



Configuration B

Figures 44–55: Movable finger lobe (MFlobe) and fixed finger socket (FFsoc) configurations in *Iurus*. *Iurus* species exhibit two distinct lobe/socket configurations: Species from the Peloponnese, Crete, Karpathos, and Rhodes comply to configuration A where the lobe and socket widths are approximately the same, exhibiting no proximal gap. Species from mainland Turkey conform to configuration B where the socket is wider than the lobe, sometimes exceeding the lobe width by a factor of two, as indicated by a conspicuous proximal gap. **44–46.** *Iurus dufourieus*, male, Peloponnese. **47.** *I. dufourieus*, female, Peloponnese. **48.** *I. sp.*, subadult male, Karpathos. **49.** *I. sp.*, male, Rhodes. **50–51.** *I. kanzelbachi*, male, Turkey. **52.** *I. kadleci*, male, Turkey. **53.** *I. asiaticus*, male, Turkey. **54–55.** *I. kraepelini*, male, Turkey.

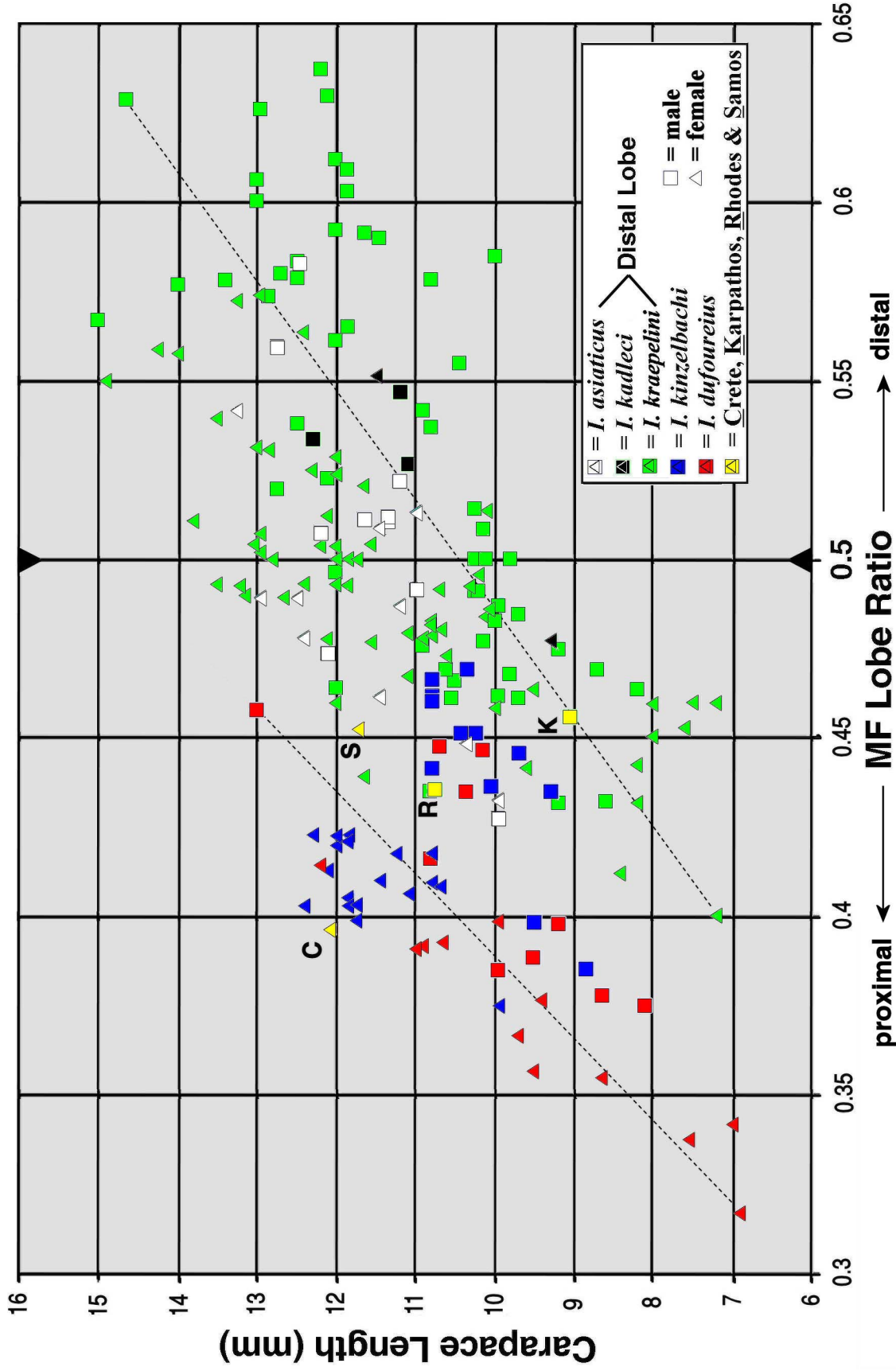


Figure 56: Scatter chart showing correspondence of movable finger lobe position with carapace length in *Iurus* species (based on 207 specimens, triangles = female, squares = male). MF lobe ratio = external condyle-to-lobe distance / MF length (i.e., a ratio of < 0.5 implies lobe is proximal of midfinger, 0.5 implies lobe is at midfinger, and > 0.5 implies lobe is distal of midfinger). Note, in particular, that the MF lobe moves distally as scorpions reach maturity in all five species (using carapace length as an indicator of maturity). Diagonal lines connecting small and large MF lobe ratios for *I. dufourei* and *I. kraepelini* highlight this observation. In general, males of comparable size have a more distal MF lobe than corresponding females in all species. Also note that in mature *I. kraepelini*, *I. kadleci*, and *I. asiaticus*, lobes are located distally, whereas *I. dufourei* and *I. kinzelbachi* lobes are located proximally. Finally, *Iurus* sp. from Rhodes exhibit proximally placed lobes as in *I. dufourei* and *I. kinzelbachi*, whereas in *I. sp.* from Karpathos (subadult) and Samos the lobe position is consistent with that in comparable specimens of *I. kraepelini*.

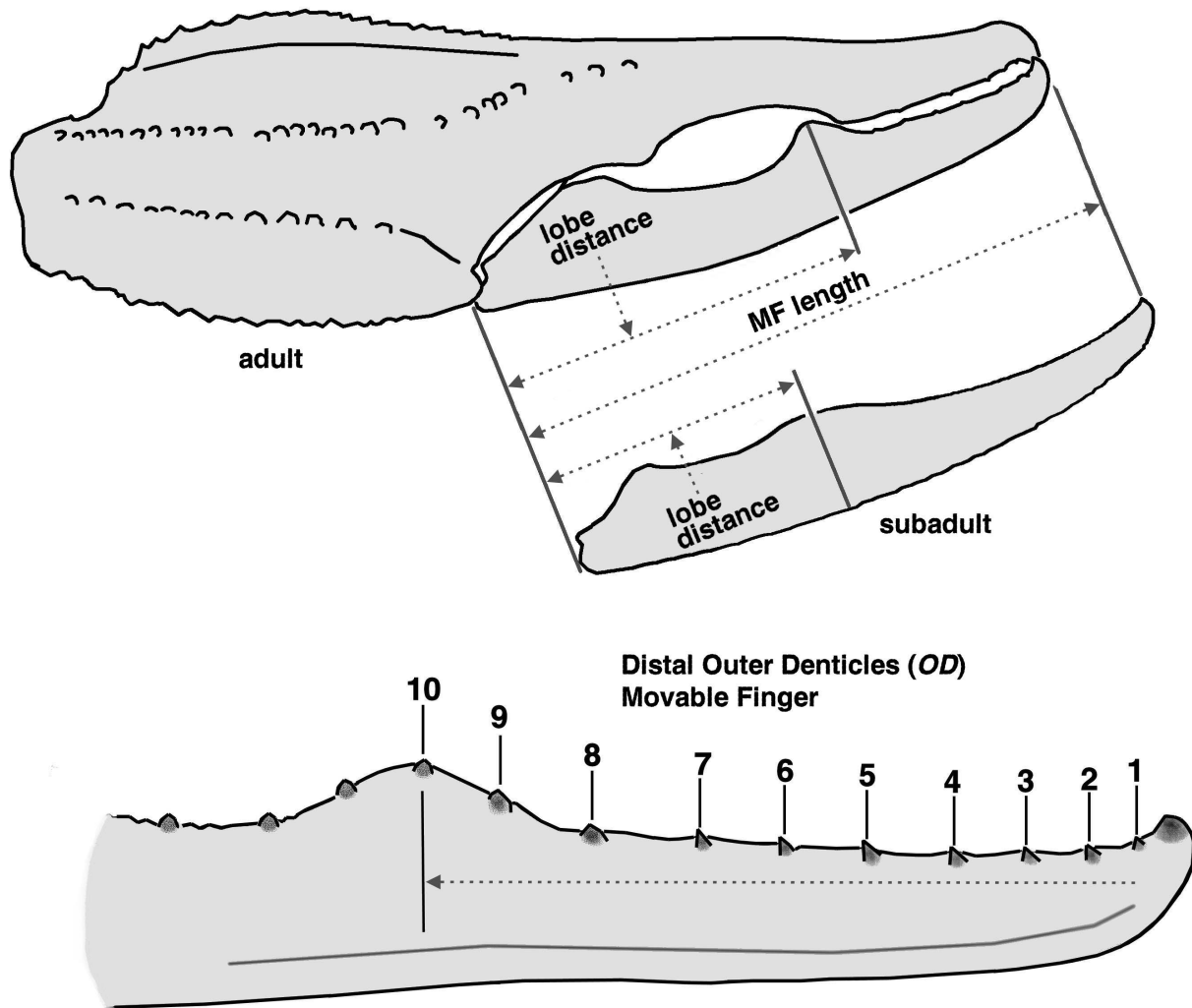


Figure 57: Conventions used in the analysis of the movable finger lobe in *Iurus*. **Top.** Method of measurement of the movable finger lobe. Lobe distance is measured from the external condyle to the center of the lobe. Movable finger lobe ratio is this distance divided by the movable finger length. Note that the finger lobe in juvenile to subadult specimens is more rounded and not as exaggerated as in adults (both are illustrated above). However, the lobe is detectable except only in the smaller juvenile specimens where the finger denticle edge is essentially straight. **Bottom.** Technique of counting the number of distal outer denticles (OD). ODs, which proximally terminate each median denticle (MD) group, are visible on the external edge of the movable finger (i.e., the MD denticle group proximal base slants externally). The “distal” OD count includes all ODs beginning from the distal denticle (DD) to the center of the movable finger lobe. By convention, if no OD occurs at the lobe center, then the closest OD occurring distally of the lobe is counted as the terminal OD.

horizontally for each carapace length partition: “red” and “blue” icons in most cases occur to the left of “green”, “black”, and “white” icons. There are very few exceptions in this 200+ sample set. *Iurus dufourei* and *I. kinzelbachi* in general exhibit a proximal MF lobe. Even the largest adults have lobe ratios less than 0.5. For example, *I. dufourei* (carapaces 12.2 and 13.0, female and male) have ratios of 0.414 and 0.458, respectively, and *I. kinzelbachi* (carapaces 12.0 to 12.4 mm, five females) exhibit ratios from 0.402 and 0.423. The largest ratios found in these two species are from male *I.*

kinzelbachi (carapaces 10.35 to 10.80), 0.460 to 0.470 (in general, males exhibit larger ratios than females, see discussion below). *Iurus kraepelini*, *I. kadleci*, and *I. asiaticus* exhibit MF lobe ratios exceeding 0.5 in most adults, especially in males. The larger specimens of *I. kraepelini* have lobe ratios exceeding 0.550 (29 specimens), nine of which exhibited 0.600 or larger. *Iurus kadleci*, **sp. nov.**, a slightly smaller species (the largest known specimen is a male with a 12.2 mm carapace), reaches ratio values up to 0.550. *Iurus asiaticus*, with lobe ratios slightly smaller than the previous two

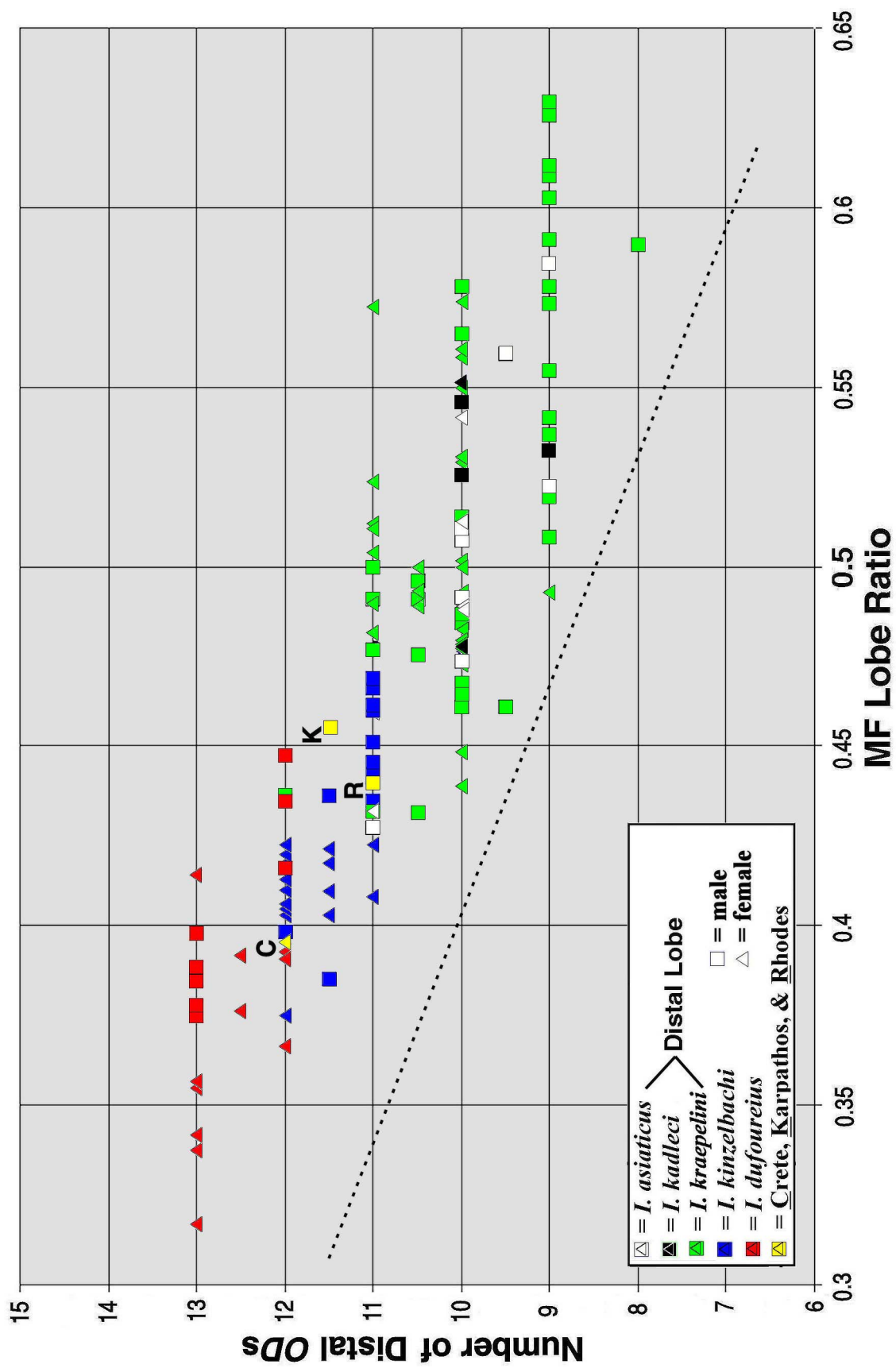


Figure 58: Scatter chart showing correspondence of movable finger lobe position with number of distal outer denticles (OD) in *Iurus* species (based on 149 specimens, triangles = female, squares = male). Number of distal ODs = number of ODs from distal denticle (DD) to lobe center (see Fig. 57); both fingers are tabulated and then averaged to produce count. Note, in particular, that the number of distal OD denticles decreases as the MF lobe moves distally. Diagonal arrow highlights this observation. See Fig. 56 for definition of MF lobe ratio.

species, ranges 0.474 to 0.584, with carapaces 12 mm or greater.

Sexual dimorphism in lobe/socket relationships.

As stated above, the proximal gap, which characterizes the two lobe/socket configurations, is almost exclusively found in sexually mature male specimens. This gap, in general, is not present, or at least is not conspicuous, in females. However, in *I. kadleci*, **sp. nov.**, the proximal gap is quite conspicuous in the large female (carapace 11.5 mm) as it is in the males. The scatter chart in Fig. 56 delineates males and females. It is clear from this chart that, in general, male specimens of a species have greater lobe ratios than females of comparable size. Again, this can be determined by inspecting the scatter chart horizontally within carapace length brackets; i.e., “triangular” icons usually occur to the left of “rectangular” icons by species.

Allometric considerations in lobe location.

Above, we demonstrated that the movable finger lobe “migrates” distally on the finger as a specimen reaches successive ontogenetic stages. The question now arises as to the dynamics of this “migration”. The distal position of the lobe is based on a ratio using the movable finger length. Therefore, an expansion of the finger base, as suggested by the proximal gap seen in configuration B, is a possible cause of this “movement”. That is, the MF lobe does not actually move distally as indicated by the ratio, but instead the ratio is impacted by the expansion of the finger bases. The other alternative is that the lobe does indeed migrate down the finger, which would also equally impact the lobe ratio. The scatter chart shown in Fig. 58 contrasts the lobe ratio with the number of distal outer denticles (*OD*) (see Fig. 57 for method of counting distal *OD*s). It is clear from this analysis that as the lobe ratio increases the number of distal *OD*s decreases. For example, in *I. dufourei*, the number of distal *OD*s ranges from 12 to 13, a count of 13 found on the specimens with the smallest lobe ratios. The same is also true of *I. kraepelini* where we see a range of 8 to 12 distal *OD*s. In most cases, counts of 8 or 9 were limited to sexually mature males only. This data implies that the MF lobe does indeed migrate distally on the finger, exhibiting less *OD*s between the lobe and the fingertip.

This same issue was discussed by Francke (1981) where he contrasted the fixed finger socket with the median denticle (*MD*) groups and finger trichobothria. We opted to use the MF lobe since it is an important taxonomic character observable in both genders throughout most ontogenetic stages.

Species differentiation based on lobe/socket/proximal gap. Figure 59 presents a “graphic key” delineating all five *Iurus* species using chelal morphology. This key is based primarily on the analysis of chelal MF lobe and proximal gap discussed in detail above. The primary couplet is the presence/absence of a

proximal gap. Only *I. dufourei* lacks a proximal gap on sexually mature males, being conspicuous in the other four species. The next key couplet is a relative position of the MF lobe, separating species by proximal or distal lobe positions. Only *I. dufourei* and *I. kinzelbachi*, **sp. nov.**, have basal lobes on sexually mature specimens; in the other three species the lobe is generally found midpoint or distally. The third couplet, curvature of the movable finger, separates *I. kraepelini* from *I. kadleci*, **sp. nov.**, and *I. asiaticus*. In *I. kraepelini*, the movable finger is curved considerably, forming a 30+° angle from its base to the distal denticle. In the other four species, this angle is smaller, roughly 20°. *Iurus asiaticus* and *I. kadleci*, **sp. nov.**, cannot be differentiated with these three characters alone (except that the proximal gap is also found in mature females in *I. kadleci*, **sp. nov.**, unique in *Iurus*).

Francke (1981: 222, figs. 3–4) discussed morphometric size differences between two sexually mature males (both had hemispermatophores, dissected by Francke) from the “same” locality, stating that “... size differences of about 30 % between these two specimens strongly suggests ... sexual maturity at different instars ...”. We have examined both of these male specimens (NHMW 11324 and NHMW 11325; photographs, illustrations, and measurements are provided for both in this paper) and, as it turns out, the “small male” is *I. asiaticus* whereas the “large male” is *I. kraepelini*. Francke quotes both males as originating from “Namrun” in Turkey; however, this is an error since only the “small male” (NHMW 11325, 16 May 1967, leg. F. Ressler) is from Namrun, now Çamlıyayla, Mersin Province, Turkey, a plateau area high in the Taurus Mountains (1100 m). The “large male” (NHMW 11324, 29 April 1967, leg. F. Ressler) is not from Çamlıyayla (= Namrun), as stated by Francke (1981), but from Göksu Valley near Silifke, Mersin, Turkey. This is one of the easternmost localities of *I. kraepelini*, a coastal area ca. 100 km southwest of Çamlıyayla, separated by a great wall of the Taurus Mts. Incidentally, these two males are easily distinguished by their chela and hemispermatophore morphology, both illustrated in the present paper.

Movable finger inner denticles (*ID*). As discussed elsewhere, determining the number of inner (*ID*) or outer (*OD*) denticles on the chelal fingers can be quite difficult in *Iurus*, especially when examining sexually mature specimens. First, the median denticle (*MD*) groups, which are oblique and highly imbricated, numbering 14 to 16, are grouped quite close to each other. On sexually mature specimens, this dentition is further obscured by movable finger lobe/fixed finger socket development. The proximal gap, if present, further complicates this issue. Typically, a precise dentition is difficult to determine at the lobe to proximal areas of the fingers. Having stated this, we still tabulated the number of *ID*s

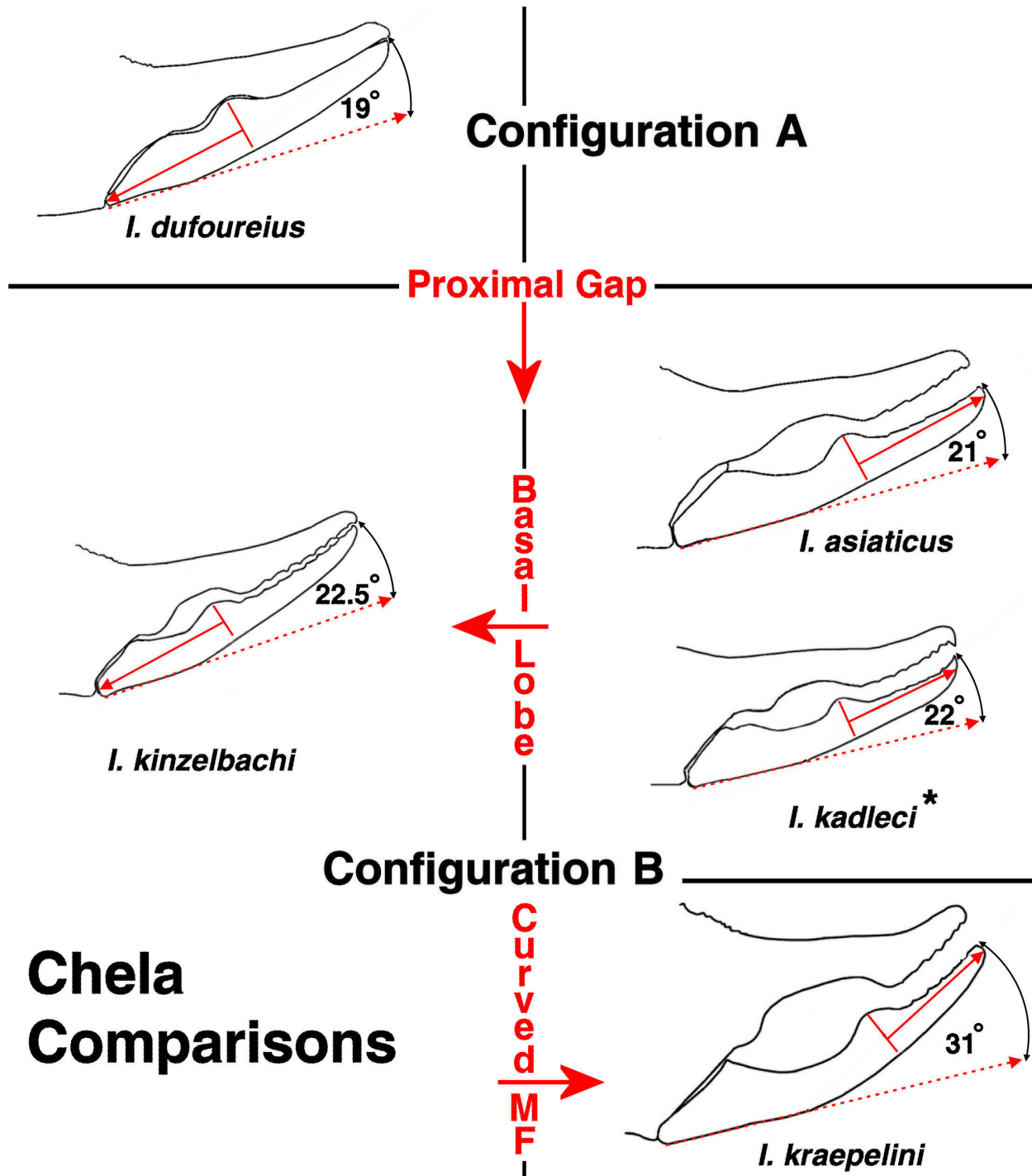


Figure 59: Chelal diagnostic differences in *Iurus* species (drawings rendered from adult males): presence/absence of proximal gap; basal/distal lobe; movable finger degree of curvature. See Figs. 44–55 for definition of terms. * Proximal gap conspicuously present in both male and female *I. kadleci* adults.

on the movable finger to establish a potential species-level diagnostic character. As can be seen from the data (Tab. 1), these *ID* counts are presented in ranges, and most data was derived from juvenile to subadult material, sexually mature specimens being ignored in

most cases for reasons just stated. We suspect that if only juvenile material was considered, the *ID* counts would be more stable, showing little variation. We also believe that the higher denticle counts probably most accurately depict the *ID* counts for the species.

	Number of <i>IDs</i>	MVD
<i>I. dufourei</i>	14–16 (14.958) (± 0.550) [24] (14.408–15.508)	> 7.1 %, 19.0 %, 28.9 %, 36.0 %
<i>I. kinzelbachi</i>	13–15 (13.966) (± 0.325) [29] (13.640–14.291)	> 11.1 %, 20.4 %, 27.0 %
<i>I. kraepelini</i>	11–14 (12.568) (± 0.691) [88] (11.877–13.260)	> 8.3 %, 14.6 %
<i>I. asiaticus</i>	11–12 (11.600) (± 0.516) [10] (11.084–12.116)	> 5.5 %
<i>I. kadleci</i>	11–11 (11.000) (± 0.000) [1] (11–11)	-

Table 1: Statistical data showing number of inner denticles (*ID*) of the chelal movable finger. Mean Value Differences (MVD) contrast largest *ID* counts with smaller counts. Statistical data group = minimum–maximum (mean) (standard deviation) [number of samples] (standard error range).

Table 1 depicts movable finger *ID* counts for 150+ specimens. Clearly, *I. dufourei* and *I. kinzelbachi* have the greater number of *IDs* within the genus, their combined means exceeding the other three species by 1.96 denticles. In the SEM micrographs of the movable fingers of *I. dufourei* (Fig. 20) and *I. kraepelini* (Fig. 19), we see 16 and 12 *IDs*, respectively, based on juvenile to subadult specimens. Interestingly, in Vachon's (1966: figs. 15–16) illustrations of the movable fingers of two *Iurus* specimens, identified as *Iurus dekanum* (Roewer) (the type specimen) and *I. dufourei*, depicted 16 and 12 *IDs*, respectively. Francke (1981), based on the chelal movable finger lobe, concluded that *I. dekanum* was probably from Greece and was *I. dufourei*. We agree with Francke's conclusion, based on the basal MF lobe, the absence of a proximal gap, and, germane to this discussion, the presence of 16 *IDs* on the movable finger. We have examined Vachon's specimen of "*I. dufourei*" from Tarsus, Mersin, Turkey, and have concluded that it belongs to *I. asiaticus* based on its chela and hemispermatophore morphology. In addition, the 12 *ID* shown in Vachon (1966: fig. 16) are consistent with our data in Table 1.

Hemispermatophore morphology

We examined 16 hemispermatophores from 13 specimens (see map in Fig. 60), representing four species. Currently, the hemispermatophore of *Iurus kadleci*, **sp. nov.**, is unknown. With the exception of *I. dufourei*, at least two specimens were examined per species, and in the case of *I. kraepelini*, six specimens. In the single studied male of *I. dufourei*, both hemispermatophores were examined. The hemispermatophore is somewhat large in *Iurus*, measuring 10.00–13.15 (11.93) (based on 12 samples). In all cases, all hemispermatophores within a species were consistent in overall morphology and relative morphometrics used for ratio calculations. Of particular interest, we see considerable differences between the four species in hemispermatophore morphology. With these differences alone we can easily differentiate the species.

All three primary components of the hemispermatophore, the trunk, median area, and lamina, are used, in part, to differentiate four *Iurus* species (Fig. 42). The trunks are essentially the same across these species except for the presence/absence of the transverse trunk bolsters (see Fig. 42). *Iurus dufourei* and *I. kinzelbachi*, **sp. nov.**, exhibit two to four sclerotized transverse trunk bolsters, whereas they are absent in *I. asiaticus* and *I. kraepelini*, **sp. nov.** The acuminate process, located in the median area, terminates with a highly tapered truncated point in all species except *I. kinzelbachi*, **sp. nov.**, whose process terminus is blunted. Since the acuminate process terminus of *Calchas* is also truncated (see discussion of this elsewhere), we hypothesize here that the blunted terminus is a derived autapomorphy for *I. kinzelbachi*, **sp. nov.** The hemispermatophore lamina provides several diagnostic differences between the four *Iurus* species. The distal portion of the lamina is either noticeably tapered forming a pointed terminus, as in *I. kraepelini* and *I. asiaticus*, or the lamina edges are essentially subparallel forming a somewhat blunted terminus, as in *I. dufourei* and *I. kinzelbachi*, **sp. nov.** The lamina internal nodule is structured differently across all four species. In *I. kinzelbachi*, **sp. nov.**, this nodule is quite subtle, rounded to obsolete. This appearance is further exaggerated by the overall elongation of the lamina and its somewhat subparallel edges. The internal nodule found in *I. dufourei* is quite conspicuous, its terminus knoblike in appearance. Although the distal portion of the lamina has subparallel edges, the internal nodule is much wider than either the distal or basal portions of the lamina. *Iurus kraepelini* has a wide rounded internal nodule, the lamina tapering considerably distally. The internal nodule of *I. asiaticus* is quite conspicuous, much wider than the lamina base, and forming a point at its terminus. These features are further exaggerated by the highly tapered and somewhat shortened distal aspect of the lamina. Finally, the lamina in *I. asiaticus* is essentially straight on its external edge, with little angling at the internal nodule apex. In the other species, the distal and basal ends of the lamina angle in an external direction, with the distal aspect in *I. kraepelini* sometimes curving back in an internal direction.